

Cite this: *RSC Adv.*, 2017, 7, 19262

# Facile fabrication of silver nanoparticle-coated silica-C18 core–shell microspheres and their applications in SERS detection†

Lin Xue,<sup>‡ab</sup> Hai-Xin Gu,<sup>‡\*b</sup> Shou-Qi Yuan<sup>\*a</sup> and Da-Wei Li<sup>ID \*c</sup>

We present a one-step method to prepare silver nanoparticle (Ag NP) shell coated functional microspheres as a surface-enhanced Raman scattering (SERS) substrate. The microspheres, linked by *n*-octadecane chains, were bonded and covered by aggregations of Ag NPs. The process of the coverage of Ag NPs on a microsphere surface was investigated by scanning electron microscopy, and the SERS activity was optimized using rhodamine 6G as a probe molecule. This spatial structure composed of inner *n*-octadecane chains and an outer coarse silver shell achieved dual functionality of molecule adsorption and sensing, due to its capacity to capture analytes with alkyl chains, thus achieving effective SERS detection with bare compacted Ag NPs. The SERS detection of low concentrations of  $2.6 \times 10^{-7}$  M,  $2.5 \times 10^{-8}$  M and  $5.4 \times 10^{-8}$  M could be achieved for naphthalene, 2,6-dimethylnaphthalene, and 1-naphthol, respectively. The prepared Ag NP shell composite microspheres would expand the range of applications for SERS, and provide an effective method for the quick SERS detection of poor-SERS-responsive molecules.

Received 20th February 2017

Accepted 21st March 2017

DOI: 10.1039/c7ra02098h

rsc.li/rsc-advances

## 1. Introduction

Coin metal (gold, silver, and copper) nanoparticles exhibit plasmonic behaviour to generate surface-enhanced Raman scattering (SERS).<sup>1–3</sup> This special optical property enables the weak Raman scattering of molecules to be enhanced by multiple orders of magnitude and provides a high sensitivity to even trace amounts of samples.<sup>4,5</sup> Hence, coin metal nanoparticles (NPs) have been of technological interest for a wide range of disciplines.<sup>6–10</sup>

However, the use of plasmonic nanoparticles may suffer from some challenges in achieving reliable applications. The SERS phenomenon strongly depends on a molecular close proximity to a metal surface where a light induced electromagnetic field is present. Therefore, the SERS effect affords a very low response to molecules that lack functional groups with affinity to metals, limiting the wide potential of SERS application. Much work has focused on the addition of functional groups onto the surface of

bare nanoparticles to capture the molecules into electromagnetic fields.<sup>11–15</sup> Unfortunately, the additional chemical groups linked to the SERS-active surface could produce Raman signals by themselves, thus complicating the identification of analytes using spectroscopy. The aggregation of nanoparticles could generate strong electromagnetic fields from the gaps between the particles and lead to a significant SERS effect on molecules thereafter. Nevertheless, the formation and distribution of the “hot spots” may be heterogeneous because of the irregular aggregation of particles, thus reducing the reproducibility and effectiveness. Moreover, it could easily result in a loss of colloidal nanoparticles during the mixing process in the sample solution due to their small size and dispersibility.

Herein, the assembled silver nanoparticle (Ag NP) shell alkyl-functionalized microspheres were fabricated to achieve high performance SERS detection with little spectral background interference. The spatial composite microspheres exhibited the dual advantages of adsorbing molecules with alkyl chains close to the bare Ag NPs surface and accomplishing high SERS-activity. Furthermore, we successfully integrated the microspheres into a small detection device suitable for on-site use, and demonstrated high sensitivity to poor-SERS-responsive molecules.

## 2. Experimental section

Details of the materials, apparatus and experiments are provided in ESI.† The schematic illustration for the experimental process is shown in Fig. 1.

<sup>a</sup>Research Center of Fluid Machinery Engineering and Technology, Jiangsu University, Zhenjiang, Jiangsu 212013, P. R. China. E-mail: shouqiy@ujs.edu.cn

<sup>b</sup>Shanghai Fire Research Institute of Ministry of Public Security, Shanghai 200438, P. R. China. E-mail: guhaixin@126.com

<sup>c</sup>Key Laboratory for Advanced Materials, Shanghai Key Laboratory of Functional Materials Chemistry, School of Chemistry and Molecular Engineering, East China University of Science and Technology, Shanghai 200237, P. R. China. E-mail: daweil@ecust.edu.cn

† Electronic supplementary information (ESI) available. See DOI: 10.1039/c7ra02098h

‡ These authors contributed equally to this work and should be considered as co-first authors.



### 3. Results and discussion

C18-functionalized microspheres are one of the commonly used substrates for absorbing and separating molecules in sample solutions. Bare Ag NPs are well-used plasmonic materials as SERS sensors.<sup>16</sup> In our experiments, the microspheres were previously modified with (3-aminopropyl) trimethoxysilane (APTMS) to facilitate the subsequent immobilization of Ag NPs onto their surfaces. The SEM image of the APTMS modified microsphere is shown in Fig. 2A. Fig. 2B–D demonstrate the process of the coverage of Ag NPs onto the bare microsphere with different assembly times. Ag NPs were initially dispersed and aggregated on the surface of the microspheres. After 7 h of deposition, the microspheres were coated with uniform and compacted Ag NP aggregations (see Fig. 2D). The EDX measurement displayed an increasing amount of Ag during the deposition process and verified the full coverage of the silver shell for the product at 7 h, as shown in Fig. 2E. The  $10^{-6}$  M probe molecule R6G was employed to investigate the SERS activity of composite microspheres that had different synthesis times. Fig. 2F shows the comparison of the SERS spectra. The SERS signals increased with the increasing coverage of Ag NPs. After the entire surface of the microsphere was covered with a dense and coarse silver shell, the SERS signals did not increase anymore. It verified that the SERS activity strongly depends on the amount of Ag NPs. These aggregated Ag NPs could effectively form particle–particle gaps to generate the strong electromagnetic fields, or “hot spots”, thus producing a remarkable SERS effect.<sup>17</sup> Besides, compared to the dispersive metallic nanoparticles in colloids, the immobilization of the Ag NPs on silicon substrates could eliminate random flowability and aggregation, thus affording stable and reproducible SERS detection. Furthermore, the SERS-active microspheres are feasible for a sample

preparation procedure such as extraction or separation in bulk solutions.

Additionally, we examined their ability of detecting non-polar molecules which traditionally have little SERS response because of their low affinity to metal surfaces. Naphthalene compounds, typical non-polar molecules, have been of great concern to public health owing to their perniciousness to the environment. Fig. 3 shows the Raman spectra of 1  $\mu$ M naphthalene acquired from three different SERS detection systems. In the Ag NP colloid system, when the molecules are located in the gaps between the particles, the strong electromagnetic fields therein would generate a remarkable enhancement of molecular signals. For the solid supported Ag NPs aggregation layer, stable and reproducible SERS detection could be obtained due to the uniform distribution of “hot spots”. However, molecular signals could hardly be observed on the Ag NP colloid and the bare silica supported Ag NP layer (see curve (i) and (ii) in Fig. 3). This illustrated the invalidation of two traditional SERS substrates for naphthalene detection, as neither the aqueous environment surrounding the silver colloids nor the bare silica support under Ag NP layer displayed any contribution to an effective SERS response. Herein, we demonstrated that the composite microspheres could achieve valid SERS detection of naphthalene (see curve (iii) in Fig. 3). In our detection system, a silica-C18–Ag NPs spatial structure was constructed. The Ag NPs were coupled with hydrophobic alkyl groups on the surface of silica microspheres. The non-polar molecules could be trapped by the alkyl chains and sandwiched between the silver layer and the supported silica substrate or the gaps of the Ag NPs. This contributed to an introduction of molecules into the electromagnetic field, thus establishing a molecular trapping-sensing system to realize high performance SERS detection. Moreover, the peak shifts in the SERS spectra were in good accordance with those in the spectra of the solid, and

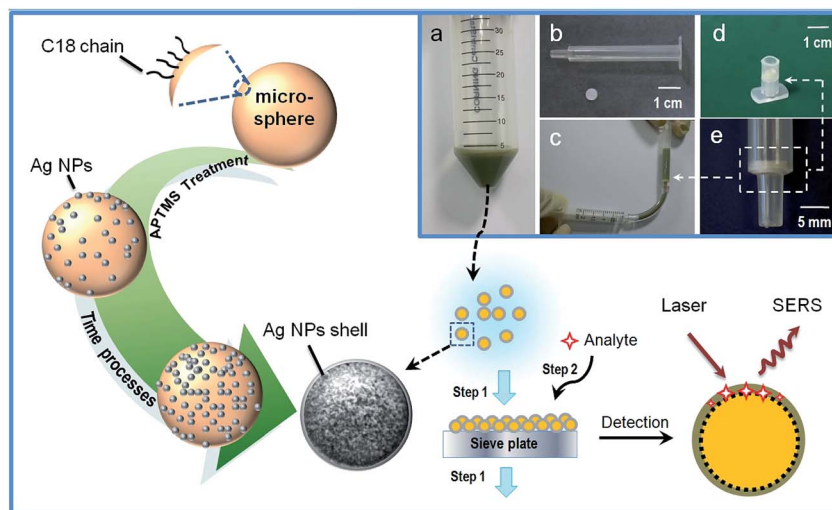


Fig. 1 Schematic illustration for the preparation of the composite microspheres and the detection of analytes. Inset: (a) a digital photo of the concentrated reaction product in a centrifuge tube; (b) a digital photo of the empty column and the rounded sieve plate; (c) operational presentation of sieving the liquid and collecting the microspheres by the assembly of the empty column and sieve plate; (d) a digital photo of a small detection device assembled with the sieve plate on the bottom; (e) a magnified photo of the sieve plate on the bottom of the column.



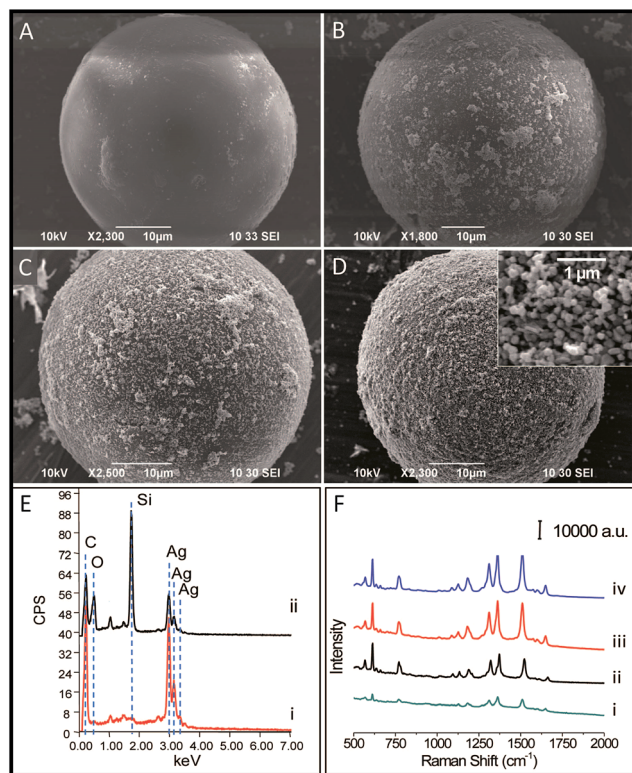


Fig. 2 SEM images of the microspheres: (A) A bare microsphere without modification with silver nanoparticles. (B) A microsphere covered with silver nanoparticles from silver colloid for 1 hour. (C) A microsphere covered with silver nanoparticles from silver colloid for 3 hours. (D) A microsphere covered with silver nanoparticles from silver colloid for 7 hours. Inset: the magnified images of Ag NP aggregations on the surface of the composite microsphere. (E) EDX spectra of the surface of the microspheres modified by silver nanoparticles for 7 hours (curve (ii)) and 3 hours (curve (i)). (F) SERS spectra of  $10^{-6}$  M R6G acquired on microspheres that were modified by silver nanoparticles for 1 hour (curve (ii)), 3 hours (curve (iii)), 7 hours (curve (iii)) and 8 hours (curve (iv)).

additional background signals were hardly observed (see curve (iii) and curve (iv) in Fig. 3). This was attributed to the Raman response of the molecule and its accessibility to the plasmonic surface. The alkyl chain with a  $-\text{CH}_3$  group on its terminus had a weak affinity to and a low interaction with the silver surface. On the other hand, the Raman cross-sections of this small molecule which lacked  $\pi-\pi$  structure are small.<sup>18</sup> Hence, the C18 group under the Ag NPs could intrinsically take advantage of averting the background signal interference compared to other reported work.<sup>11–15</sup>

In order to demonstrate the potential for practical use, naphthalene, 2,6-dimethylnaphthalene, and 1-naphthol at different concentrations were tested by our detection device, as shown in Fig. 4. Their corresponding concentrations were characterized by the signal intensities of the peaks located at  $1377\text{ cm}^{-1}$ ,  $1374\text{ cm}^{-1}$ , and  $1367\text{ cm}^{-1}$  respectively. The insets show the relationship between the intensities of the characterized peaks of the compounds and their respective logarithmic concentrations. The signal intensities decreased gradually in response to decreasing concentrations, and low

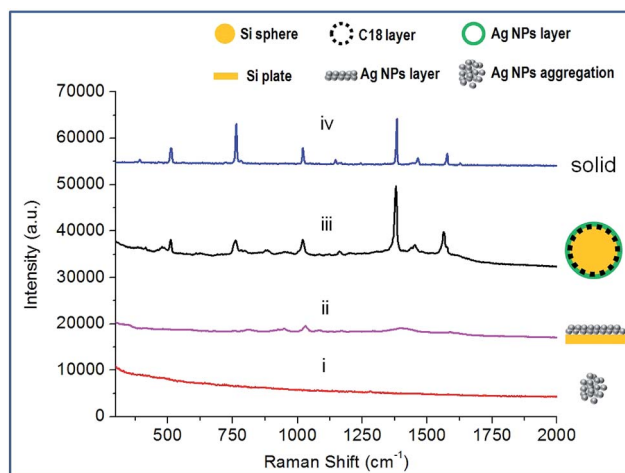


Fig. 3 Comparison spectra of  $10^{-6}$  M naphthalene obtained from three different SERS detection substrates: the silver nanoparticle colloid (curve (i)), the silver nanoparticle layer modified silicon plate (curve (ii)), and the silver nanoparticle shell composite microspheres (curve (iii)). Curve (iv) was obtained from solid naphthalene.

concentrations down to  $2.6 \times 10^{-7}$  M,  $2.5 \times 10^{-8}$  M and  $5.4 \times 10^{-8}$  M were achieved for naphthalene (see Fig. 4A), 2,6-dimethylnaphthalene (see Fig. 4B), and 1-naphthol (see Fig. 4C) respectively. This demonstrated that the prepared composite microspheres and the device could realize high performance detection of naphthalenes. Compared to other reported work (Table S1†), the SERS-active microspheres possessed a comprehensive advantage in terms of their sensitivity to naphthalenes, ease of preparation, elimination of background interference and capability of on-site use for bulk solutions.

In view of the satisfactory results for each single compound, we further investigated the potential of the composite microspheres in real-world conditions. The soil (from Shanghai Fire Research Institute of MPS, Shanghai, China) was used as a common carrier of the naphthalenes. The soil was immersed and extracted with ethanol to stimulate background conditions in a real sample. The spectrum of the extracted solution was obtained by our detection device, as shown in Fig. 5a. It demonstrated that the amount of naphthalenes in the soil itself was lower than the limit of detection and that the analysis would not be significantly interfered with by the background spectrum from the extracted solution. In order to investigate the validity in real sample conditions, an equal amount of naphthalene, 2,6-dimethylnaphthalene, and 1-naphthol was added into the extracted solution and each compound at a final concentration of  $1\text{ }\mu\text{M}$  was prepared. Every single compound in the mixture could be confirmed according to the positions of the SERS peaks (see Fig. 5b). This demonstrates the feasibility and ability of the SERS-active composite microspheres to effectively detect naphthalenes in real-world conditions, even for a complicated and multi-composition sample.



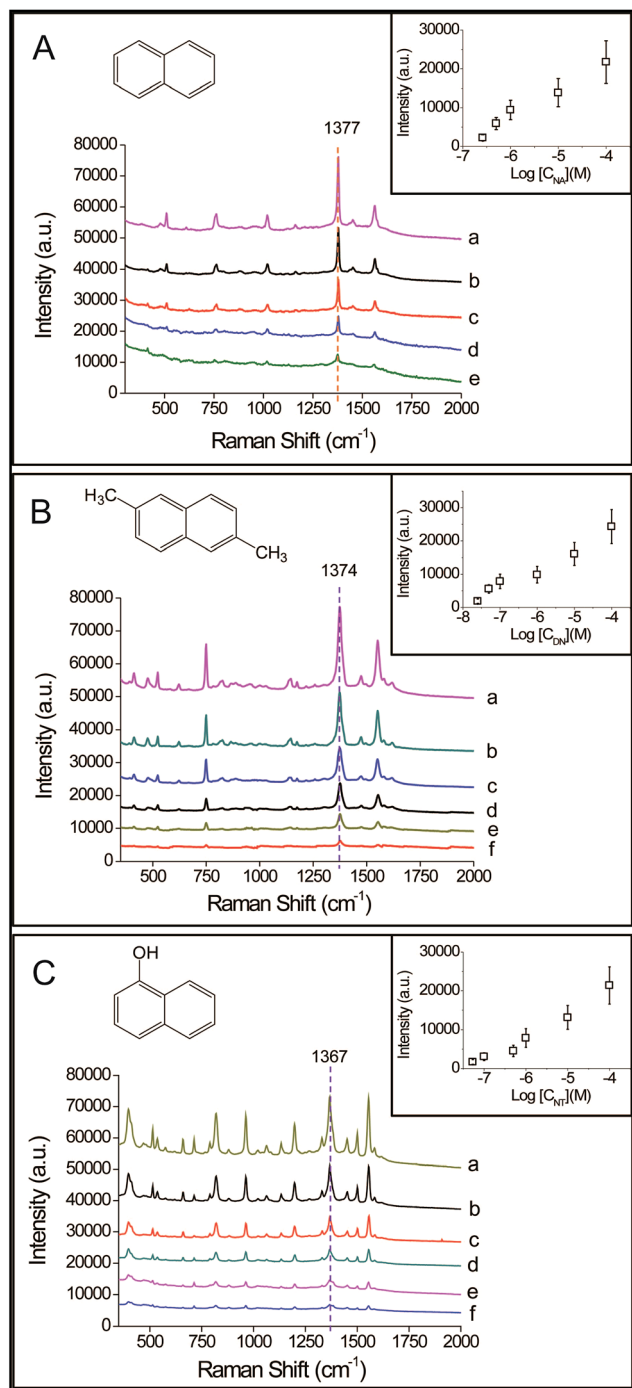


Fig. 4 (A) SERS spectra of naphthalene at different concentrations of (a)  $1 \times 10^{-4}$  M, (b)  $1 \times 10^{-5}$  M, (c)  $1 \times 10^{-6}$  M, (d)  $5 \times 10^{-7}$  M, (e)  $2.6 \times 10^{-7}$  M. The inset shows a plot of signal intensity vs. logarithmic naphthalene concentration for the band at  $1377 \text{ cm}^{-1}$ . (B) SERS spectra of 2,6-dimethylnaphthalene at different concentrations of (a)  $1 \times 10^{-4}$  M, (b)  $1 \times 10^{-5}$  M, (c)  $1 \times 10^{-6}$  M, (d)  $1 \times 10^{-7}$  M, (e)  $5 \times 10^{-8}$  M, (f)  $2.5 \times 10^{-8}$  M. The inset shows a plot of signal intensity vs. logarithmic 2,6-dimethylnaphthalene concentration for the band at  $1374 \text{ cm}^{-1}$ . (C) SERS spectra of 1-naphthol at different concentrations of (a)  $1 \times 10^{-4}$  M, (b)  $1 \times 10^{-5}$  M, (c)  $1 \times 10^{-6}$  M, (d)  $5 \times 10^{-7}$  M, (e)  $1 \times 10^{-7}$  M, (f)  $5.4 \times 10^{-8}$  M. The inset shows a plot of signal intensity vs. logarithmic 1-naphthol concentration for the band at  $1367 \text{ cm}^{-1}$ . The molecule structures correspond to naphthalene, 2,6-dimethylnaphthalene and 1-naphthol respectively.

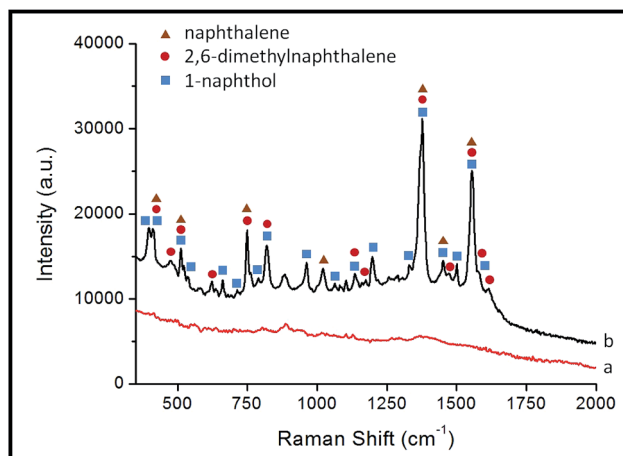


Fig. 5 (a) The Raman spectrum of the extracted solution from soil. (b) The SERS spectrum of the extracted solution mixed with naphthalene, 2,6-dimethylnaphthalene, and 1-naphthol. The symbols marked on the peaks correspond to the respective compounds.

## 4. Conclusion

In summary, we prepared composite microspheres with silica-C18 cores and silver nanoparticle shells as a SERS substrate. The spatial structure of the microsphere gave rise to a molecular trapping-sensing system to capture the molecules into intense electromagnetic fields and achieve an effective SERS detection. A highly sensitive and background-interference-free SERS measurement for non-polar molecules like naphthalenes was demonstrated. Therefore, it would provide a promising method for SERS detection of molecules which intrinsically have a poor SERS response, and extend the potential of SERS for wide application.

## Acknowledgements

This work was sponsored by Natural Science Foundation of Shanghai (14ZR1409400, 14ZR1410800), Scientific Research Project of MPS (2016JSYJB34, YJ20163202), and National Key Natural Science Foundation (Grant No. 51239005).

## Notes and references

- 1 F. P. Zamborini, L. Bao and R. Dasari, *Anal. Chem.*, 2012, **84**, 541.
- 2 S. Fateixa, H. I. S. Nogueira and T. Trindade, *Phys. Chem. Chem. Phys.*, 2015, **17**, 21046.
- 3 S. Schlücker, *Angew. Chem., Int. Ed.*, 2014, **53**, 4756.
- 4 S. Nie and S. R. Emory, *Science*, 1997, **275**, 1102.
- 5 J. F. Li, Y. F. Huang, Y. Ding, Z. L. Yang, S. B. Li, X. S. Zhou, F. R. Fan, W. Zhang, Z. Y. Zhou, D. Y. Wu, B. Ren, Z. L. Wang and Z. Q. Tian, *Nature*, 2010, **464**, 392.
- 6 Z. Han, H. Liu, J. Meng, L. Yang, J. Liu and J. Liu, *Anal. Chem.*, 2015, **87**, 9500.
- 7 X. Bi, X. Du, J. Jiang and X. Huang, *Anal. Chem.*, 2015, **87**, 2016.



- 8 G. Soliveri, S. Ardizzone, S. Yüksel, D. Cialla-May, J. Popp, U. S. Schubert and S. Hoepfner, *J. Phys. Chem. C*, 2016, **120**, 1237.
- 9 C. Muehlethaler, M. Leona and J. R. Lombardi, *Forensic Sci. Int.*, 2016, **268**, 1.
- 10 P. Liou, F. X. Nayigiziki, F. Kong, A. Mustapha and M. Lin, *Carbohydr. Polym.*, 2017, **157**, 643.
- 11 Y. H. Kwon, K. Sowoidnich, H. Schmidt and H. D. Kronfeldt, *J. Raman Spectrosc.*, 2012, **43**, 1003.
- 12 L. Guerrini, J. V. Garcia-Ramos, C. Domingo and S. Sanchez-Cortes, *Anal. Chem.*, 2009, **81**, 1418.
- 13 L. Yang, L. Ma, G. Chen, J. Liu and Z. Q. Tian, *Chem.–Eur. J.*, 2010, **16**, 12683.
- 14 K. Gracie, D. Lindsay, D. Grahama and K. Faulds, *Anal. Methods*, 2015, **7**, 1269.
- 15 S. S. R. Dasary, Y. K. Jones, S. L. Barnes, P. C. Ray and A. K. Singh, *Sens. Actuators, B*, 2016, **224**, 65.
- 16 P. C. Lee and D. Meisel, *J. Phys. Chem.*, 1982, **86**, 3391.
- 17 Y. Fang, N. H. Seong and D. D. Dlott, *Science*, 2008, **321**, 388.
- 18 R. A. Alvarez-Puebla and L. M. Liz-Marzán, *Angew. Chem., Int. Ed.*, 2012, **51**, 11214.

